2019 Rock Dynamics Summit– Aydan et al. (eds)
© 2019 Taylor & Francis Group, London, ISBN 978-0-367-34783-3

Dynamic shear strength of an artificial rock joint under cyclic and seismic wave loading

T. Okada
Central Research Institute of Electric Power Industry, Chiba, Japan

T. Naya
Dia Consultants Co., Ltd., Saitama, Japan

ABSTRACT: Static strength has traditionally been considered as rock strength in the foundation bedrock for seismic design in Japan. The appropriate evaluation of dynamic strength instead of static strength became necessary for dynamic response analysis following the Great East Japan Earthquake. Therefore, we previously proposed a mathematical model to evaluate the dynamic strength for intact rocks. In this study, we performed laboratory tests and validated the model for discontinuity by using an artificial rock. As a result, the dynamic strength exceeded the static strength in the experimental and calculated results. However, the influence of fatigue and loading rate were less, compared to the cases of intact rocks. Therefore, the dynamic strength of the discontinuity does not greatly differ from static strength.

1 INTRODUCTION

In seismic design for the foundation bedrock of nuclear power plants in Japan, static strength has traditionally been used as rock strength, based on the fact that "dynamic strength ≧ static strength". This relationship has been validated for various rock types (Nishi & Esashi 1982, Yoshinaka et al.1987, Sugiyama et al. 2001). However, those test conditions are limited. Dynamic strength does not have a clear definition. Besides, it is difficult to formulate a single definition of dynamic strength because seismic waveforms are diverse, and the stress waveform inside the ground also varies depending on the location. To resolve these issues, we proposed a mathematical model to evaluate dynamic strength (Okada & Naya 2018). Using the mathematical model, the dynamic strength can be obtained by monotonic loading tests performed at several loading rates in different orders and cyclic loading tests at several different shear stress amplitudes. In the previous research, we performed laboratory tests to validate the model, using intact rocks, but we have never conducted the test using rock joints.

In this study, monotonic loading and cyclic loading direct shear tests were conducted on the artificial rock joint we made from plaster in order to obtain the parameters of the mathematical model. Afterwards, multistep direct shear tests under cyclic and seismic-wave loadings were performed, followed by simulations using the mathematical model. The test results showed that the dynamic strength exceeds the static strength, corroborating previous research. Furthermore, the dynamic strength calculated from the mathematical model of the artificial rock joint was generally consistent with the dynamic strength obtained from the experimental data.

2 MATHEMATICAL MODEL OUTLINE OF DYNAMIC STRENGTH

2.1 *Effect of fatigue*

When the stress amplitude is fixed, and repeated stress is applied until the failure of specimen, the stress amplitude decreases as the number of cycles increases. This relationship is called stress-cycle (S-N) curve in the field of designing the fatigue strength of metallic materials. The function expressing this relationship is defined as the fatigue function f_1 and is expressed as follows:

$$f_1\left(N_f\right) := \frac{\tau_{f\_N_f}}{\tau_{f\_N=1}} = 1 - a \cdot \log N_f \qquad (1)$$

where N_f (≧1) is the number of cycles at the time of failure, τ_{f_Nf} is the shear strength at the time of failure following the loading N_f, $\tau_{f\_N=1}$ is the shear strength under monotonic loading (N=1), and a is a parameter defining the slope of the function, which means that the decrease in strength is greater for larger values of a. To simplify the problem, confining pressure is not considered in this function.

2.2 *Effect of loading rate*

It is also known that strength tends to increase as loading rate increases. While the fatigue effect always leads to decrease in the strength as the number of cycles increases, increasing the loading rate tends

to increase the strength. In our proposed mathematical model, the relationship between the dynamic and static strengths is determined mainly by these two effects. We define the function f_2 as the function that represents the relationship between the loading rate and shear strength, and define it as follows:

$$f_2(\dot{\varepsilon}) := \tau_f = \alpha + \beta \cdot \log \dot{\varepsilon} \tag{2}$$

where $\dot{\varepsilon}$ is the axial strain rate (%/min), τ_f is the maximum shear strength (MPa), and α and β are parameters. To simplify the problem, the confining pressure is not considered in this function.

2.3 *Integration of fatigue and loading rate effects*

Letting τ_f in Eq. (2) be the strength $\tau_{f\_N=1}$ at loading time N = 1 in Eq. (1), the following relationship is obtained:

$$\tau_{f\_N_f} = f_1 \cdot f_2 = (\alpha + \beta \cdot \log \dot{\varepsilon})(1 - a \cdot \log N_f) \tag{3}$$

From this relationship, the relationship between $N_f(\geqq 1)$and τ_{f_Nf} at any strain rate can be obtained. Note that the derivation of Eq. (3) assumes that the relation in Eq. (1) is satisfied, regardless of the loading rate. However, experimental data confirms that this assumption is, to some extent, reasonable (Okada & Ito 2009).

2.4 *Application of cumulative damage rule*

To express the impact of an arbitrary waveform in the mathematical model, it is necessary to know the impact of the cyclic loading that leads to fracture (hereinafter referred to as the "damage effect"). However, because no such test data was available, we applied the cumulative damage rule used in metal materials design (Otaki 2007). The strength exerted after N wave loading (hereinafter referred to as "residual strength") is assumed to change linearly with respect to its fracture count. Adopting this perspective, the damage function f_3 representing the damage effect due to cyclic loading can be expressed as follows:

$$f_3(N) := \frac{\tau_{d\_N}}{\tau_{f\_N=1}} = 1 - d \cdot (N - 1) \tag{4}$$

where N is the number of cycles preceding failure, and τ_{d_N} is the strength (residual strength) exerted after N cycles. At the time of failure (when $N=N_f$), Eq. (1) = Eq. (4) obtains. Because $f_1(N_f) = f_3(N_f)$, the following relation is obtained:

$$d = \frac{a \cdot \log N_f}{N_f - 1} = \frac{1 - \dfrac{\tau_{f\_N_f}}{\tau_{f\_N=1}}}{\dfrac{1 - \dfrac{\tau_{f\_N_f}}{\tau_{f\_N=1}}}{10^{\frac{}{a}}} - 1} \tag{5}$$

Therefore, the parameter d in Eq. (4) is determined from Eq. (5) when the stress ratio $\dfrac{\tau_{f\_N_f}}{\tau_{f\_N=1}}$ is determined. The following relationship is then obtained from Eqs. (2) and (4):

$$\tau_{f\_N_f} = f_2 \cdot f_3 = (\alpha + \beta \log \dot{\varepsilon})\{1 - d(N - 1)\} \tag{6}$$

Note that for Eq. (6) to hold in the manner of Eq. (3), the relationship shown in Eq. (4) must hold, regardless of the loading rate. Lacking empirical data in this regard, we make the same assumptions as the cumulative damage rule. This assumption makes it possible to determine the degree of damage even if the stress ratio $\dfrac{\tau_{f\_N_f}}{\tau_{f\_N=1}}$ is determined at different loading rates.

3 VALIDATION OF THE DYNAMIC STRENGTH CALCULATED FROM THE MODEL

3.1 *Specimens*

An artificial rock discontinuity was used as the test specimen in order to validate the numerical model with fewer variations of geometric and mechanical properties. The discontinuity was made by using a mold that has a regular protruding ridge with an angle of 30 degrees (Figure 1); that is a simulated rocked discontinuity. The discontinuous plane is 200 mm long (shear direction) and 100 mm wide, and the height of the protruding ridge is about 4 mm.

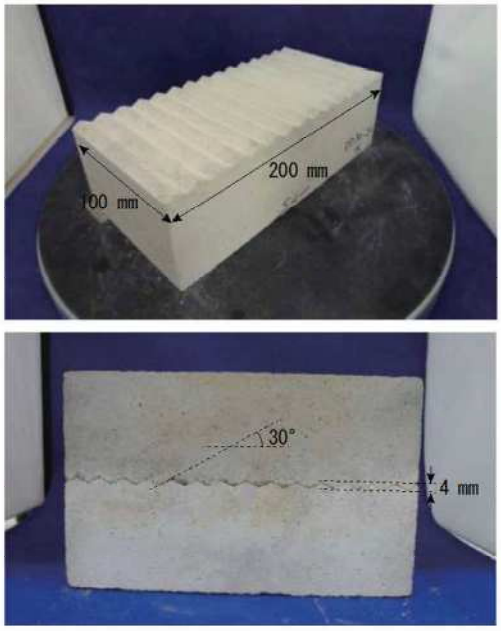

Figure 1. Specimen of discontinuity of artificial rock.

Furthermore, intact specimens with no discontinuity and a discontinuity with an angle of 0 degree (horizontal surface) were made.

The compound ratio of the sand, clay, cement and water of the artificial rock was 67.1:6.9:11.2:14.8 by weight. The curing period of the material was set between 30 to 42 days in order to reduce the variations in the mechanical properties. The wet density was about 1.9 g/cm^3 and the unconfined compressive strength was about 14 MPa.

3.2 *Test equipment*

The direct shear test equipment with two-axis hydraulic servo-type actuators was used for all the tests (Figure 2). A hydraulic cylinder is electrically controlled by a hydraulic servo valve and the load-cell output value is fed back for control. Both the maximum vertical load and shear load are 200 kN. The friction of the vertical and shear load is reduced by a crosshead and linear guide respectively. The structure of the shear box is shown in Figure 3. The pressure plate is not separated from the shear box and is part of the upper box according to the JGS0561 method (Japanese Geotechnical Society 2009). A defect of this shear box is that as loading progress, the gap between the upper and lower (movable) box changes, and, as a result, the thickness of the shear plane varies from the initial value. The initial gap before the vertical loading was fixed at 6 mm in order to ensure that it would be greater than the height of the protruding ridge after the vertical loading.

3.3 *Test method*

Direct shear tests were carried out in principles corresponding to the standard method for direct shear test on a rock joint (Japanese Geotechnical Society, 2009). A list of purposes and loading conditions is given in Table 1.

Series D30-1 represents the monotonic loading test, and the asssumed static strength test. The displacement rate was 0.05 mm/min, and the vertical

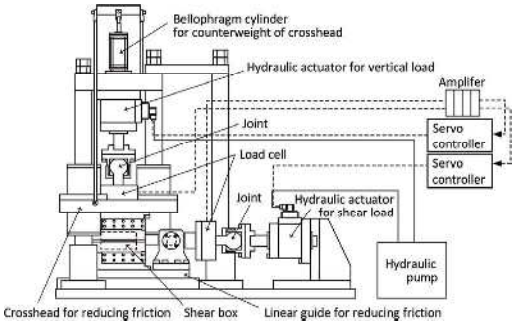

Figure 2. The direct shear test equipment

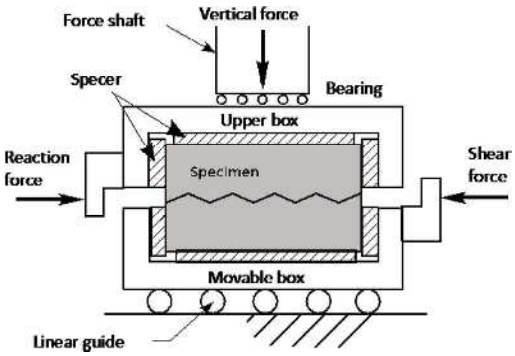

Figure 3. The direct shear box.

stress ranged from 0.2 MPa to 6.0 MPa. Intact specimens with no discontinuity and discontinuities with an angle of 0 degree (horizontal surface) were also used for comparative test. Series D30-2 represents the cyclic loading tests for investigating the fatigue function. The loading frequencies were 0.1 Hz and the waveforms were sine waves. Vertical stress was fixed at 0.2 MPa. Series D30-3 represents the monotonic loading tests for investigating the loading rate function. They were performed at various displacement rates (0.05–15 mm/min). Series D30-4 represents the multistep cyclic loading test for validating the dynamic strength evaluation model. D30-4a and D30-4b represent the sine and seismic wave loading,

Table 1. Information on the direct shear tests

Series	Purpose	Loading method	Loading conditions				Vertical stress (MPa)	Quantity (pcs)
D30-1	Static strength	Monotonic	Displacement rate: 0.05mm/min				0.2 to 6.0	4
D30-2	Fatigue effect	Cyclic	Frequency: 0.1 Hz, Stress amplitude: 1.6 to 2.0 MPa				0.2	6
D30-3	Rate effect	Monotonic	Displacement rate: 0.005 to 15 mm/min				0.2	4
D30-4a	Model validation	Multistep Cyclic	No.	Frequency (Hz)	Waves (cycles)	Number of steps	0.2	3
			D30-4a1	0.1	10	10		
			D30-4a2	0.01	50	10		
			D30-4a3	0.1	5	5		
D30-4b			No.	Seismic wave		Number of steps	0.2	2
			D30-4b1	Time axis 50 times		5		
			D30-4a1	Time axis 20 times		5		

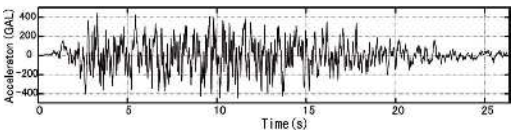

Figure 4. Artificial seismic wave.

respectively. The frequency, number of waves, and number of steps are as indicated in Table 1. In D30-4b, an artificial seismic wave was used, as shown in Figure 4, and the time axis was stretched about 20 or 50 times, owing to the limitations of the shear loading actuator of the test machine.

3.4 *Test results*

(1) Static Strength

The static strength characteristics obtained from D30-1 are shown in Figure 5 with the results of the intact specimen and the discontinuity with an angle of 0-degree (horizontal surface). The result of the intact and 0-degree discontinuity yielded values of $\phi \fallingdotseq 40°$. The 0 and 30-degree discontinuities yielded vales of $c \fallingdotseq 0$. When 30-degree discontinuity having values of $\phi \fallingdotseq 40°$ slides on its surface, the value of the friction angle theoretically becomes 70 degrees. Although the friction angle of the test of the 30-degree discontinuity is nonlinear, the friction angle is 64 degrees at low confining pressure. The value is slightly lower than 70 degrees, but it is a reasonable value, in consideration of a small breakage of the surface of the discontinuity. The value of the friction angle of the 30-degree discontinuity becomes about 40 degrees at high confining pressure because of the complete destruction of the surface.

(2) Fatigue tests

Examples of the results of the fatigue test on 30D-2 are shown in Figure 6. The shear displacement increases as loading progresses, and then, they sharply increase at 680 seconds once the shear stress can no longer be maintained. All the fatigue tests show the specific point at which shear displacement rapidly increases. These points were defined as failure points and were counted and recorded as the number of cycles leading up to failure N_f.

Figure 7 shows that the relationship between N_f and the strength normalized with the strength at single wave loading. This relationship corresponds to Eq. (1). The equation approximated using the least square method is shown as a solid line in the figure. The three data that the number of cycles exceeds 1000 times did not show the failure, however the data were assumed as the failure data for approximation using the least square method. Therefore, the actual gradient of the straight line is less steep than that in the figure. The parameter value for Eq. (1) was $a = 0.0288$.

The impact of fatigue on the discontinuity was considerably smaller, compared to the case of intact rocks (Okada & Naya, 2018).

(3) Loading rate function from the tests

The relationship between loading rate and shear strength obtained in D30-3 is shown in Figure 8. Note that the loading rate on the horizontal axis is the shear displacement rate (mm/min). These relationships correspond to Eq. (2). Further, the dispersion of the test data is small. The equation approximated by the least square method is shown as a solid line in the figure. The parameter value for Eq. (2) was $\alpha = 0.441$ and $\beta = 0.00872$. α is the strength at a displacement rate of 1 mm/min. The β/α implied rate of strength gain was

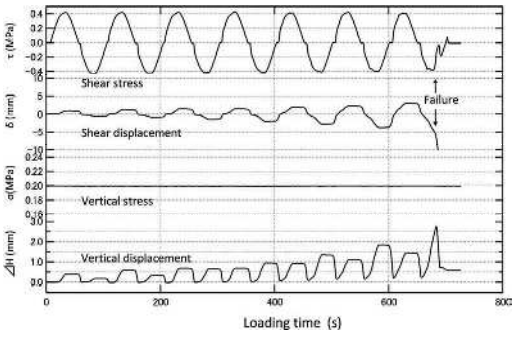

Figure 6. Static strength characteristics.

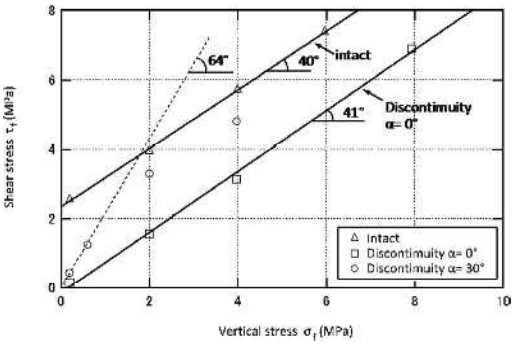

Figure 5. Static strength characteristics.

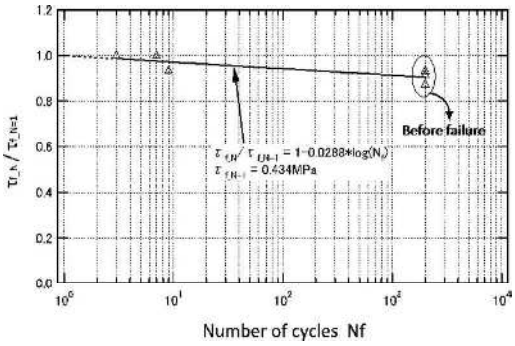

Figure 7. Fatigue test results.

0.02. The value was considerably lower than the value for intact rocks (Okada & Naya, 2018).

(4) Multiple step loading tests for validation

Figure 9(a) and Figure 9(b)M show examples of the test results for the sine and seismic wave multistep cyclic loading in the cases of D30-4a3 and D30-4b2. As both loading progresses, the shear displacement gradually increases. Then, the shear displacement rapidly increases when shear stress amplitude can no longer be maintained. In all cases, the specific point at which shear displacement rapidly increases was clear. These points were defined as failure points, and the maximum shear stress provided before the failure points were designated the strength at multi-step cyclic loading, that is, the dynamic strength.

3.5 *Discussion*

The dynamic strength was obtained from the multistep cyclic test and then compared with the calculation results obtained by the evaluation model. The static strength is assumed to be the strength at the loading rate of 0.05 mm/min as shown in Figure 8.

The static strength should be determined from Figure 5, but the strength characteristics were nonlinear, and the strength was affected by the approximate nonlinear function.

The calculation of the sine wave loading rate, using the mathematical model proceeds in the following manner: letting the loading time be the time required for N = 1/4 of a sine wave, the shear displacement at the point of failure can be considered an almost constant value, regardless of the loading rate (Figure 10). The loading rate at failure was calculated from the loading frequency and the failure displacement. Under the present conditions where the shear stress increases at the same frequency, the lower the stress amplitude, the lower the displacement rate. Therefore, when the stress amplitude is 1/n, the loading rate is also calculated as 1/n.

The calculation of the seismic wave loading rate using the mathematical model proceeds in the following manner (Figure 11): the point where the seismic wave crosses the X axis (Y=0) is identified, and the time interval (Tn) is obtained for each half wave. In the same manner as for the sine wave, the shear displacement in relation to the failure rate was calculated. If the seismic wave time axis is stretched by 10 times, the displacement rate will be 1/10. When the stress amplitude is 1/n, the loading rate is also calculated as 1/n. In addition, as shown in Figure 11, letting the respective stress histories be the maximum value on both the positive and negative sides, the dynamic strength is calculated separately for each side using the mathematical model, and the side with the maximum absolute value is taken as the dynamic strength.

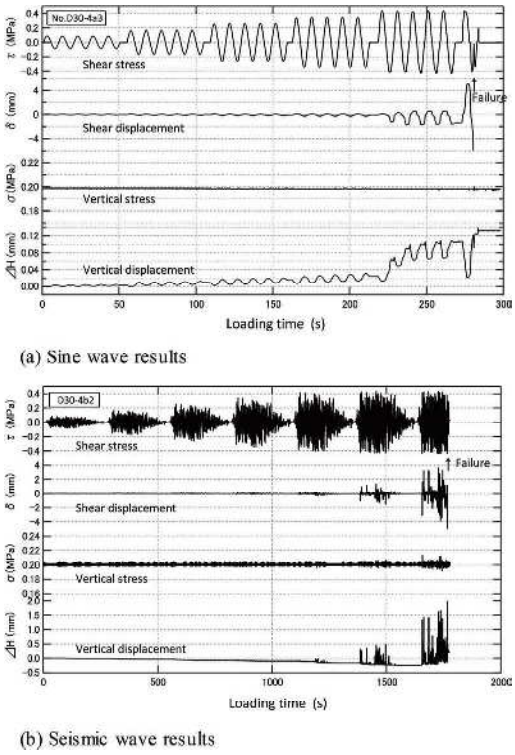

Figure 9. Examples of multistep cyclic loading tests.

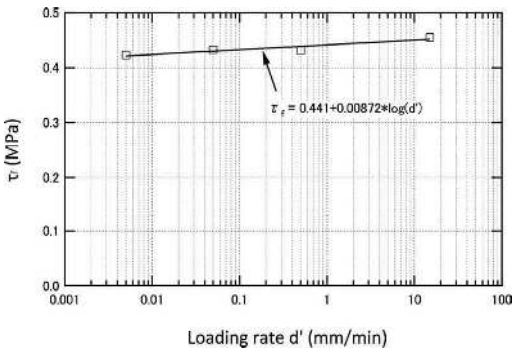

Figure 8. Loading rate function from the tests.

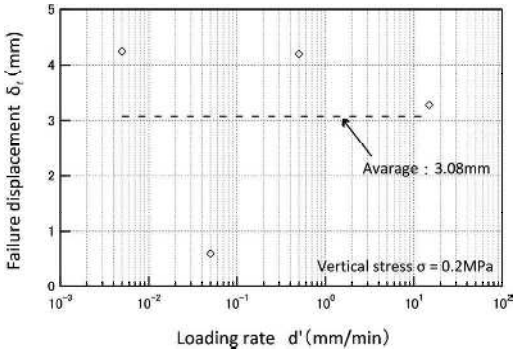

Figure 10. Failure displacement at various loading rate.

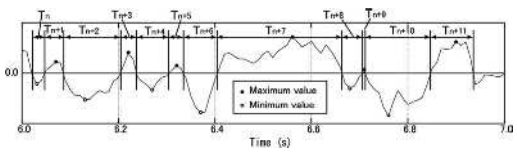

Figure 11. Illustration of frequency and stress history in a seismic wave.

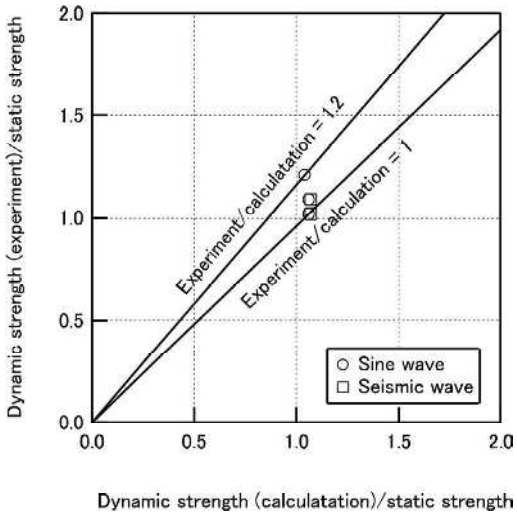

Figure 12. Comparison between experimental and calculated results.

Figure 12 shows the relationship between the dynamic strength obtained from the calculation and the dynamic strength obtained from the experiment normalized with the static strength. On the vertical axis, the dynamic strength (experiment)/ static strength ranges from 1.02 to 1.09. On the horizontal axis, the dynamic strength (calculated)/static strength is from 1.02 to 1.07. The dynamic strength is larger than the static strength in the experimental and calculated results. Comparing the experimental and calculated results, the experimental results range from -4–16%. The relative error does not greatly differ from the value for intact rocks (Okada & Naya, 2018). However, the impact of fatigue and loading rate were small; therefore, the influence of variation was relatively large. As a result, the dynamic strength of the discontinuity does not greatly differ from the static strength.

4 CONCLUSION

(1) We had proposed a mathematical model to evaluate the dynamic strength for intact rocks in the previous research. We performed laboratory tests and validated the model for discontinuity by using an artificial rock.
(2) The dynamic strength is larger than the static strength in the experimental and calculated results. However, the influence of fatigue and loading rate were less, compared the case of intact rocks. Therefore, the dynamic strength of the discontinuity does not greatly differ from its static strength.
(3) We plan to conduct laboratory tests in order to get experimental results for cyclic loading of large number of cycles under extreme loading conditions and high loading rate to further clarify the dynamic strength of rock discontinuities.

REFERENCES

Japanese Geotechnical Society. 2009. Method for direct shear test on a rock discontinuity, *Geotechnical materials test methods and commentary*: 912–944 (in Japanese).

Nishi,K. and Esashi, Y.1982. Study on the mechanical properties of mudstone (Part 4), *Central Research Institute of Electric Power Industry Research Report* 382014 (in Japanese).

Okada, T. and Ito, H. 2009. Mathematical modeling of the dynamic strength of soft rock, *Proc. the 38th Symposium on Rock Mechanics* (in Japanese).

Okada, T. and Naya, T. 2018. A mathematical model for evaluating the dynamic shear strength of rock and validation of the model with laboratory test data, *Proc. 3rd Int. Conf. on Rock Dynamics and Applications, Trondheim*: 179–185.

Otaki, H. 2007. Mechanical fatigue strength design method, Nikkan Kogyo Shimbun (in Japanese).

Sugiyama,H, Saotome, A. and Nakamura, Y. 2001. Dynamic strength characteristics of volcanic breccia based on triaxial compression test, *The 56th Annual Scientific Lecture Meeting of the Japan Society of Civil Engineers*: 134–135 (in Japanese).

Yoshinaka, R., Ogino, I., Takada,S. and Kanazawa, K.1987. Strength characteristics of sedimentary soft rock under dynamic cyclic loading, *7th National Symposium on Rock Mechanics in Japan technical papers*: 61–66 (in Japanese).